Penerbit Akademia Baru

Journal of Advanced Research in Fluid Mechanics and Thermal Sciences

Journal homepage: www.akademiabaru.com/arfmts.html
ISSN: 2289-7879

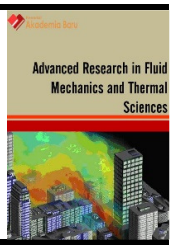

A Comparison of Openflume Turbine Designs with Specific Speeds (*Ns*) Based on Power and Discharge Functions

Open Access

Sanjaya Baroar Sakti Nasution[1,*], Warjito[1], Budiarso[1], Dendy Adanta[1]

[1] Department of Mechanical Engineering, Faculty of Engineering, Universitas Indonesia, 16424 Depok, Indonesia

ARTICLE INFO

Article history:
Received 12 April 2018
Received in revised form 20 July 2018
Accepted 24 July 2018
Available online 6 November 2018

ABSTRACT

Openflume turbines have more stability and efficiency than other types of turbines, such as Pelton, Turgo, undershot, breastshot, overshot and cross-flow turbines, because openflume turbines have wider non-dimensional *Ns* ranges. The design of an openflume turbine blade depends on *Ns* parameters: power function and discharge function. In this study, two openflume turbines were designed with these parameters to determine which was best. With analytical calculations, two runner geometries, A and B, were designed based on discharge and power functions, respectively, and further developed and tested. The runners had the same numbers of blades but different angles of attack. The calculations predicted that Runner A would produce 735.08 W of power, and runner B would produce 1037.77 W of power. However, in numerical simulations, runner A produced 656.29 W of power, and runner B produced 874.49 W of power. Based on those methods runner B was more efficient than runner A. Based on the analytical designs, runner B was manufactured and tested. The power it produced was 868.69 W. The differences between the experiment and numerical results, in terms of efficiency, were not significant. Thus, the numerical simulation was valid. Consequently, the design of an openflume turbine runner should be based on *Ns* power functions.

Keywords:
pico hydro, openflume, specific speed

Copyright © 2018 PENERBIT AKADEMIA BARU - All rights reserved

1. Introduction

In 2015, 15.65% of the population of Indonesia (37,190,668 people) did not receive electricity because the distribution of hydro was difficult due to geographical conditions [1]. Pico hydro turbines can prevent such problems. The investment and generation cost is lower than wind turbines and solar PV technology [2]. In addition, pico hydro also has the lowest life cycle cost (LCC) [3].

Pico hydro turbines are water turbine with maximum powers of 5 kW [4]. There are several types of pico hydro turbines, such as openflume, propeller, undershot, breastshot, overshot, Archimedes, Pelton, Turgo and Francis turbines. Openflume turbine is propeller turbine with open spiral cases. Openflume turbine has more stability and efficiency than other types of turbines because his *Ns* ranges, which can be based on power functions (Ns_P), is wider; i.e., the ranges are 400–1,000 RPM/s [6]. Therefore, openflume turbines are recommended for use in remote areas of Indonesia.

Many studies of openflume turbines were conducted. For example, At-Tasneem *et al.,* [7] investigated the effects of flow rates on pico hydro turbines' performances, and modified the pumps

* *Corresponding author.*
E-mail address: sanjayabaroarnasution@gmail.com (Sanjaya Baroar Sakti Nasution)

of such turbines into propellers. Moreover, Ridzuan *et al.,* [8] conducted a study of whether pico hydro turbines could be used as alternatives to power plants, and Masjuri *et al.,* [9] varied the angles and numbers of turbine propeller blades using the computational fluid dynamic (CFD) method to understand the dominant effects of these variables.

Additionally, Adhikari *et al.,* [10] designed and built a pico hydro turbine with a five-blade runner as an electrification effort in Nepal. Arrieta *et al.,* [11] observed what was received by a blade to prevent the blade from breaking, and Stamp and Susanto [12] identified ways to install pico hydro turbines; results showed that the standing method is better than the lying and angling methods. Moreover, Alexander *et al.,* [13] designed blades with four variations of *Ns* to determine the variable's relationship with power; it was found that an *Ns* of 242 provides the best hydraulic efficiency with openflume turbines.

Singh and Nestmann [14] conducted a detailed experiment regarding the effects of exit blade geometry on the part-load performances of low head–axial flow propeller turbines. Singh and Nestmann [15] also investigated the sizes and numbers of blades of turbines to determine which size and which number of blades were generated the most power. Moreover, Budiarso *et al.,* [16] designed an openflume turbine by creating a hub–tip ratio (d_h/D) of 0.4 with the free-vortex theory and analyses.

Other studies [16,17] showed that the design of an openflume turbine blade depends on *Ns* parameters. That is, for openflume turbines, there are two *Ns* parameters that are often used to design runners. They are power and discharge functions. The two different parameters require different runner design geometries, especially in regards to numbers of blades and d_h/D; the different runner designs affect the performances of runners [16,17].

The literature review above shows there were no studies of *Ns* that compared the two parameters. To fill this gap and determine which one is the best for openflume turbines, this study compared two runners, A and B. Runner A was designed based on discharge functions, and runner B was designed based on power functions. Three methods were used—analytical, numerical and experimental—to obtain runner performance characteristics.

2. Methodology

2.1 Analytical Method

When designing an openflume turbine, *Ns* is used as a parameter to determine the d_h/D and number of blades of the turbine. *Ns* is the speed a turbine needs to produce one unit of power at a height of one unit [19]. *Ns* based on a power function [17] is as follows.

$$Ns_P = \frac{N\sqrt{P}}{H^{\frac{5}{4}}} \tag{1}$$

The relationship between d_h/D, number of blades, and Ns_P is shown in Table 1.

Table 1
Numbers of blades and d_h/D based on *Ns*, which is based on power functions [5]

Variable	Value					
Number of Blades	3	4	5	6	8	10
d_h/D	0.3	0.4	0.5	0.55	0.6	0.7
Ns	1000	800	600	400	350	300

Ns based on a discharge function [17] is as follows.

$$Ns_Q = \frac{N\sqrt{Q}}{H^{\frac{3}{4}}} \tag{2}$$

Figure 1 presents a graph with *Ns*, used to determine a turbine's number of blades based on *Ns* discharge functions.

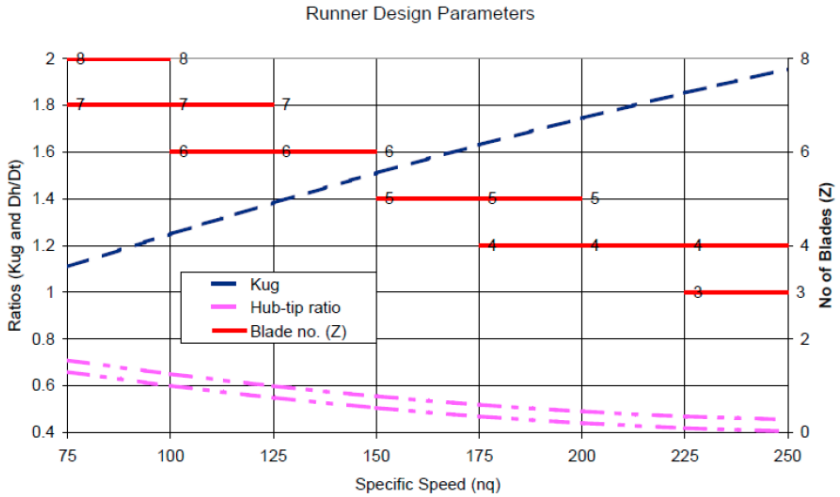

Fig. 1. A graph of the numbers of blades and d_h/D of a turbine based on *Ns* discharge functions [17]

In addition to the aforementioned variables, the velocity triangle theory is used to determine the turbine's runner dimensions, including the runner's relative velocity, absolute velocity and angle of attack. The turbine's optimum power is based on the Euler power equation. Figure 2 is a schematic drawing of the velocity triangles of an openflume turbine.

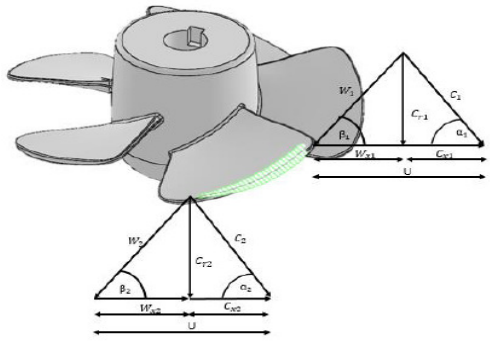

Fig. 2. A velocity-triangle analysis

Turbine power is a dependent variable related to the total torque and the rotation of a runner. Runner torque is caused by lift and drag force on the surface of a runner's blade. Such force results from interactions between the flow of a fluid and the blade's surface. A fluid flows over the blade's surface and generates lift force (F_L) and drag force (F_D), which are calculated using the lift and drag coefficients C_L and C_D, respectively, and the flat-plate theory [19].

$$F_L = \frac{1}{2} C_L \rho A W^2 \quad (3)$$

$$F_D = \frac{1}{2} C_D \rho A W^2 \quad (4)$$

$$T = \Sigma(F_L \cos\beta_1 - F_D \sin\beta_1)\, r \quad (5)$$

$$P = T\, x\, \omega = \frac{T\, x 2\pi\, N}{60} \quad (6)$$

2.2 Numerical Method

Computational methods were used to determine what parameter resulted in the best runner performance in this study. The computational process began with building a three-dimensional model of each runner. Then, each model was tested using CFD analyses. Standard k-epsilon models were used to predict turbulent flow. To determine the appropriate number of meshes for the models, a mesh independency test was carried out with the categories coarse, medium and fine.

2.3 Experimental Method

The aforementioned analytical method was used to design the two runners. The calculations were based on runner heads of 2.71 m and runner discharges of 0.041 m^3/s. Runners A and B had tip diameters of 0.124 m and hubs of 0.05 m, as well as six blades. Additionally, the runners had penstock heights and widths of 0.6 m and 0.4 m, respectively. For draft tubes, PVC pipes with diameters of 6 m and lengths of 2 m were used.

Moreover, a three-phase induction motor generator with a power of 1 horse power (HP), a maximum rotation of 1,400 RPM and full-load maximum efficiency of 74% was used. The output power of the generator was obtained by measuring the amperes and voltages of the generator using the power factor of the generator. The power factor depended on the specifications of the generator. The power factor of generator used was 0.77 at full load.

An experimental method was then used to validate the numerical method (testing was performed on the only most efficient runner, runner B). The experiment's setup is shown in Figure 3. The data obtained for and with this method were divided into two categories: primary data and secondary data. Primary data were obtained during the experiment, while secondary data were obtained from other sources. Mass flow rate, electric voltage, electric current, torque and shaft rotation were the primary data, and flow friction on the runner's draft tube and on the runner's penstock were secondary data. Primary data collection was done in two ways: through automatically logging data directly into a computer (10 variables each second) and through retrieving data manually (as many as 50 variables).

The floating method was used to calculate discharge. That is, the surface velocity of water was multiplied by a correction factor to obtain an average water velocity that depended on the depth and the type the of water channel [20] used for the turbine for which the runner was constructed. Measurements of discharge were made for five segments; each segment was 120 cm length and 40 cm wide. Then, the average discharge was calculated; it was the sum of the discharges of each segment divided by the number of segments.

Finally, a DT-2235B model tachometer was used to measure the turbine's rotation speed; it had an accuracy of 0.05% and a maximum rotation per minute of 1,999. Moreover, load cells were used to determine the magnitude of the torque on the turbine's shaft. Subsequently, 10 variables were collected every second for one minute, with an accuracy of 0.02%.

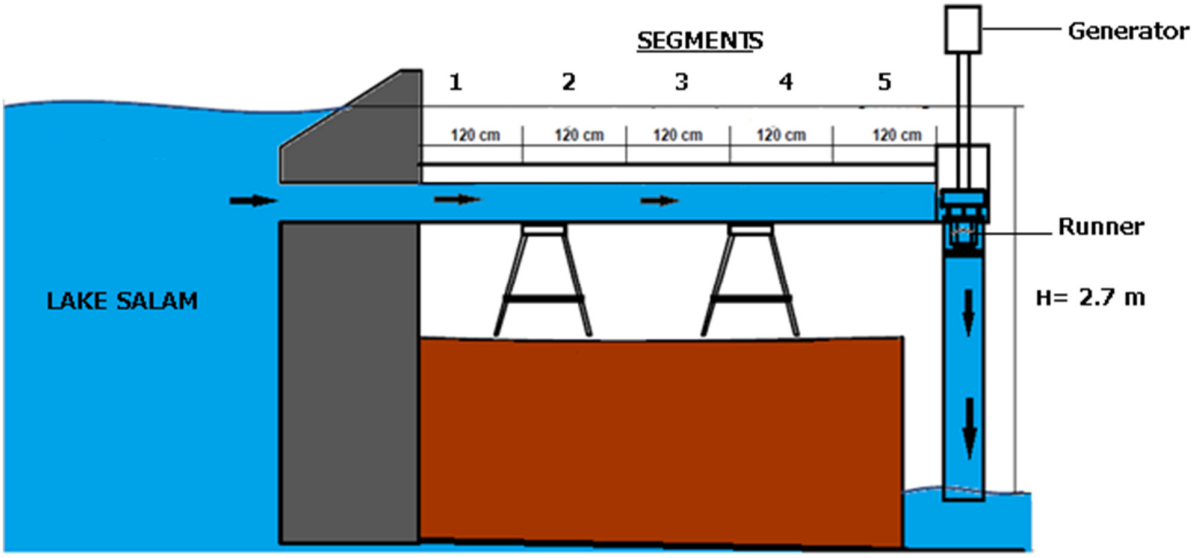

Fig. 3. A schematic of the experiment's setup

3. Results

3.1 Analytical Results

Triangle velocity analyses were conducted for each runner (based on discharge and power function); seven points were used that increased by *dh/D* from 0.4 to 1. This was done to maintain a constant rotation velocity along the runners' blades. Tables 2 and 3 show the dimensions of the runners based on the triangle velocity analyses.

Table 2
Runner A's dimensions with an specific speed with discharge function of 144.2.

d_h/D	U	C_r	C_x	θ_2	β_2	θ_3	β_3	Airfoil
0.4	4.56 m/s	3.31 m/s	4.29 m/s	4.51^0	85.48^0	10.72^0	79.28^0	4,421
0.5	5.7 m/s	3.31 m/s	3.44 m/s	34.32^0	55.67^0	13.31^0	76.69^0	4,418
0.6	6.84 m/s	3.31 m/s	2.86 m/s	50.19^0	39.81^0	15.85^0	74.15^0	4,415
0.7	7.98 m/s	3.31 m/s	2.45 m/s	59.05^0	30.95^0	18.33^0	71.67^0	4,412
0.8	9.12 m/s	3.31 m/s	2.14 m/s	64.58^0	25.42^0	20.73^0	69.27^0	2,412
0.9	10.26 m/s	3.31 m/s	1.91 m/s	68.36^0	21.64^0	23.06^0	66.94^0	2,409
1	11.4 m/s	3.31 m/s	1.71 m/s	71.11^0	18.89^0	25.32^0	64.68^0	2,406

Table 3
Runner B's dimensions with an specific speed with power function of 451.23 rad/s.

d_h/D	U	C_r	C_x	θ_2	β_2	θ_3	β_3	Airfoil
0.4	3.89 m/s	4.06 m/s	-4.82 m/s	64.44^0	46.36^0	-37.05^0	17.8^0	6,506
0.5	4.87 m/s	4.06 m/s	-3.6 m/s	64.44^0	37.32^0	-37.05^0	17.5^0	6,406
0.6	5.84 m/s	4.06 m/s	-2.78 m/s	64.44^0	30.92^0	-44.32^0	17.32^0	6,306
0.7	6.81 m/s	4.06 m/s	-2.2 m/s	64.44^0	26.25^0	-51.01^0	16.78^0	4,506
0.8	7.79 m/s	4.06 m/s	-1.76 m/s	64.44^0	22.74^0	-57.04^0	15.89^0	4,409
0.9	8.76 m/s	4.06 m/s	-1.42 m/s	64.44^0	20.02^0	-62.38^0	14.95^0	4,309
1	9.73 m/s	4.06 m/s	-1.15 m/s	64.44^0	17.86^0	-67.08^0	14.02^0	2,412

Visual representations of Tables 2 and 3 can be seen in Figures 4 and 5. Stagger angles were used to determine each blade's angle of attack, which is a function of lift and drag force on a blade. Angle of attack variations were used to determine types of airfoil and to ensure the turbine's rotation was balanced; lift and drag force imbalance can cause a blade to vibrate, and cavitation can occur. Figure 6 shows the distributions of lift and drag force on runners A and B. The lift force on runner B was higher overall, but from runner B's centre to hub, the force was lower than that of runner A.

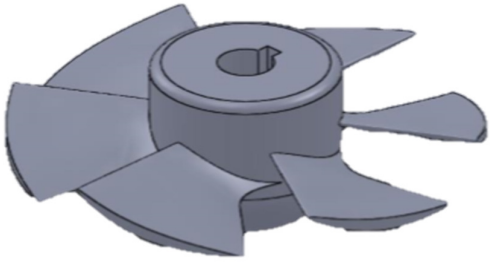

Fig. 4. Runner A

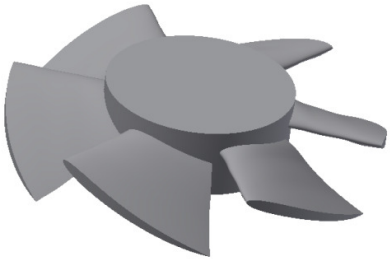

Fig. 5. Runner B

Moreover, the drag force on runners A and B did not differ significantly except on the runners' hubs. However, it should be noted that the total force received by runner A was lower than that of runner B. This may have occurred because the distribution of lift and drag force on runner A was too steep; when the force accumulated, it had a low value. However, considering the results that were obtained (Tables 2 and 3 and Figure 6), runner B performed better than runner A; B produced 1037.77 W with a torque of 6.61 Nm, and A produced 735.80 W with torque of 4.68 Nm. This analysis was based on Equations (3)–(6).

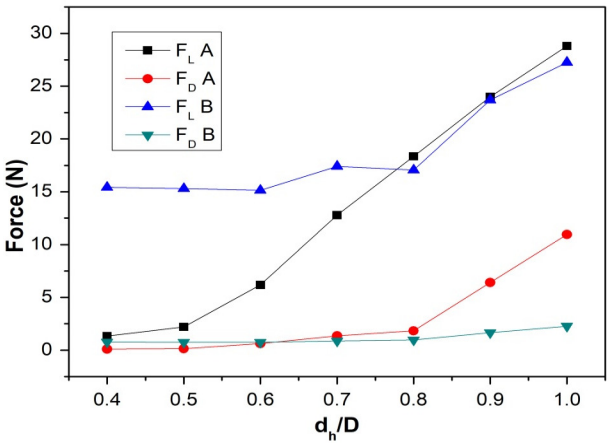

Fig. 6. Lift and drag force produced by runner A and B

3.2 Numerical Results

To determine the number of meshes needed for the model with minimal errors, a mesh independency test was conducted by finding the velocity at y = 1.5 m below the runner. Three different mesh types and amounts were used: coarse (100,000), medium (200,000) and fine (300,000). The results showed that models with 200,000 and 300,000 meshes were similar, so for this study, 200,000 were used. Table 4 presents a comparison of the analytical results and simulations using runners A and B.

Table 4
The performances of Runners A and B

Runner type	Power (analytical)	Power (numerical)	Efficiency (analytical)	Efficiency (numerical)
Runner A	735.08 W	656.29 W	62.45%	55.76%
Runner B	1037.77 W	874.49 W	95.20%	74.30%

Table 4 shows that runner B was more efficient than runner A in both the analytical and numerical results. A study conducted by Adhikari *et al.,* [10] had similar results. The researchers designed runner using *Ns* based on discharge functions. In the study, the runner's efficiency was 53.82%, and it is similar to runner A; 55.76%. Moreover, Alexander *et al.,* [13] found similar results to runner B. The researchers designed runners using *Ns* based on power functions; the result was a runner with an efficiency of over 70%.

3.3 Experiment Results

As aforementioned, runner B was more efficient than runner A. Thus, runner B was manufactured and tested. The results showed that the average discharge of each segment of the runner was 0.053 m^3/s. Moreover, the correction factor was 0.85, so the discharge was 0.045 m3/s.

Figure 7 shows that the discharges decreased from segment one to segment five. This was due to friction losses along the penstock of the runner. Friction losses caused the water's velocity to reduce, so the time the water took to reach a position close to the turbine was long.

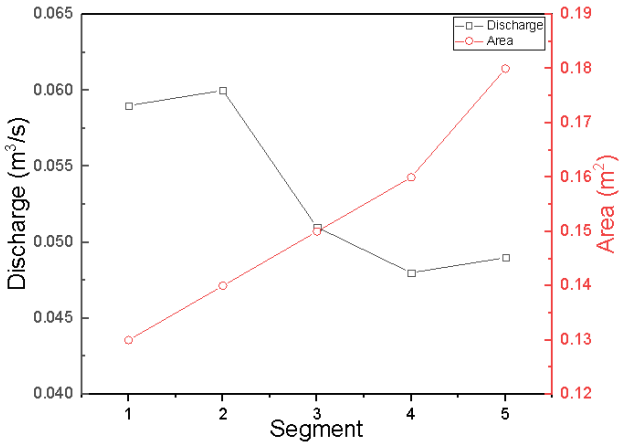

Fig. 7. The segments' discharges and areas

In addition, the results showed that the runner had a mechanical power of 868.69 ± 22 W and a torque of 2,486 ± 0.016 Nm. The runner also had a turbine spin speed of 3,338 ± 16.98 RPM and an efficiency of 73.8%. From the experiment result above, the differences between experiment and simulation results, in regards to efficiency, were not significant, so the numerical method was valid.

4. Conclusions

The designs of the two runners, each with an *Ns* based on either a power or discharge function, had the same numbers of blades but different angles of attack. The analytical and numerical analyses showed that runner B, with Ns based on a power function, was better than runner A. This was because the distributions of lift and drag force on runner A increased from hub to tip; consequently,

the accumulation of force was lower than that of runner B. Moreover, there was a difference in the angles of attack of the two runners that impacted by absolute velocity inlet (Cr_1). However, as the difference was not significant, the torque of runner B (generated mathematically) was more influenced by lift and drag coefficients. Thus, each openflume turbine runner design should have an *Ns* based on a power function (Ns_p).

Acknowledgement
This research was funded by a grant from the Directorate of Research and Community Service (DRPM) Universitas Indonesia, grant no 2403/UN2.R3.1/HKP.0.5.00/2018

References

[1] Energi, Direktorat Jenderal Ketenagalistrikan Kementerian, and Sumber Daya Mineral. "Statistik Ketenagalistrikan 2015." *Diakses dari http://www. djk. esdm. go. id/pdf/Buku% 20Statistik% 20Ketenagalistrikan/Statistik% 20Ketenagalistrikan% 20T. A* 202016.
[2] Ho-Yan, Bryan. "Design of a low head pico hydro turbine for rural electrification in Cameroon." PhD diss., 2012.
[3] Dendy Adanta, "Aplikasi Model Turbulen pada Turbin Piko Hidro," Universitas Indonesia, 2017.
[4] Williams, Arthur, and Stephen Porter. "Comparison of hydropower options for developing countries with regard to the environmental, social and economic aspects." *Small* 1 (2006): 10MW.
[5] Nechleba, Miroslav. "Hydraulic turbines, their design and equipement." (1957).
[6] Williamson, S. J., B. H. Stark, and J. D. Booker. "Low head pico hydro turbine selection using a multi-criteria analysis." *Renewable Energy* 61 (2014): 43-50.
[7] At-Tasneem, Mohd Amin, Azam Wan Mohamad, and Jamaludin Ummu Kulthum. "A study on the effect of flow rate on the power generated by a pico hydro power turbine." *World Applied Sciences Journal* (2014): 420-423.
[8] Ridzuan, Mohd Jamir Mohd, S. M. Hafis, K. Azduwin, K. M. Firdaus, and Zawawi Zarina. "Development of pico-hydro turbine for domestic use." *Appl Mech Mater* 695 (2014): 408-12.
[9] Othman, Masjuri Musa, Juhari Ab Razak, Mohd Farriz Bashar, Nor Salim Muhammad, and Kamaruzzaman Sopian. "CFD Analysis on The Flat Runner Blades of Propeller's Turbine under Low Head and Low Flow Condition." *Applied Mechanics & Materials* 699 (2014).
[10] Adhikari, Pradhumna, Umesh Budhathoki, Shiva Raj Timilsina, Saurav Manandhar, and Tri Ratna Bajracharya. "A Study on Developing Pico Propeller Turbine for Low Head Micro Hydropower Plants in Nepal." *Journal of the Institute of Engineering* 9, no. 1 (2014): 36-53.
[11] Arrieta, Chica, Edwin Lenin, Sergio Agudelo Flórez, and Natalia Isabel Sierra. "Application of CFD to the design of the runner of a propeller turbine for small hydroelectric power plants." *Revista Facultad de Ingeniería Universidad de Antioquia* 69 (2013): 181-192.
[12] Susanto, J., and S. Stamp. "Local installation methods for low head pico-hydropower in the Lao PDR." *Renewable energy* 44 (2012): 439-447.
[13] Alexander, K. V., E. P. Giddens, and A. M. Fuller. "Axial-flow turbines for low head microhydro systems." *Renewable Energy* 34, no. 1 (2009): 35-47.
[14] Singh, Punit, and Franz Nestmann. "Exit blade geometry and part-load performance of small axial flow propeller turbines: An experimental investigation." *Experimental Thermal and Fluid Science* 34, no. 6 (2010): 798-811.
[15] Singh, Punit, and Franz Nestmann. "Experimental investigation of the influence of blade height and blade number on the performance of low head axial flow turbines." *Renewable Energy* 36, no. 1 (2011): 272-281.
[16] Budiarso, M. Ridho, Reza Dianofitra, "Optimasi Turbin Mikrohidro untuk Daerah Terpencil:Openflume," *SNTTM*, 2014.
[17] Simpson, R. G., and A. A. Williams. "Application of computational fluid dynamics to the design of pico propeller turbines." In *Proceedings of the international conference on renewable energy for developing countries*. University of the District of Columbia Washington, DC, 2006.
[18] Harinaldi, Budiarso, *Sistem Fluida: Prinsip Dasar dan Penerapan Mesin Fluida, Sistem Hidrolik, dan Sistem Pneumatik*. Jakarta: Erlangga, 2015.
[19] Wright, A. K., and D. H. Wood. "The starting and low wind speed behaviour of a small horizontal axis wind turbine." *Journal of Wind Engineering and Industrial Aerodynamics* 92, no. 14-15 (2004): 1265-1279.
[20] *Manual for Micro-Hydro Power Development*. Jakarta: Japan International Cooperation Agency.